AMP-activated protein kinase activation ameliorates eicosanoid dysregulation in high-fat–induced kidney disease in mice

Anne-Emilie Declèves[1,2]*, Anna V. Mathew[3]*, Aaron M. Armando[4], Xianlin Han[5], Edward A. Dennis[4,6], Oswald Quehenberger[4,7] and Kumar Sharma[1,8].

[1]Institute of Metabolomic Medicine, University of California San Diego; [2]Laboratory of Metabolic and Molecular Biochemistry, Faculty of Medicine, Université of Mons; [3]Division of Nephrology, Department of Internal Medicine, University of Michigan; [4]Department of Pharmacology, University of California, San Diego; [5]Barshop Institute of Aging, Department of Medicine, University of Texas Health San Antonio, [6]Department of Chemistry and Biochemistry, University of California, San Diego; [7]Department of Medicine, University of California, San Diego; [8]Center for Renal Precision Medicine, Division of Nephrology, Department of Medicine, University of Texas Health San Antonio.

Running title: AMPK ameliorates eicosanoids in HFD-induced CKD

*These authors contributed equally to this work.

Corresponding author:

Anne-Emilie Declèves, PhD
Research Institute for Health Sciences and Technology
Laboratory of Metabolic and Molecular Biochemistry, Faculty of Medicine
8, Avenue du Champ de Mars
7000 Mons, Belgium
Phone number: 0032-477-914430
anne-emilie.decleves@umons.ac.be

Keywords: Obesity, eicosanoids, chronic kidney disease, high fat diet, AMPK, AICAR

ABSTRACT

High-fat diet (HFD) causes renal lipotoxicity that is ameliorated with AMPK activation. Although bioactive eicosanoids increase with HFD and are essential in regulation of renal disease, their role in the inflammatory response to HFD-induced kidney disease and their modulation by AMPK activation remain unexplored. In a mouse model, we explored the effects of HFD on eicosanoid synthesis and the role of AMPK activation in ameliorating these changes. We used targeted lipidomic profiling with quantitative mass spectrometry to determine PUFA and eicosanoid content in kidneys, urine, renal arterial and venous circulation. HFD increased phospholipase expression as well as the total and free pro-inflammatory AA and anti-inflammatory DHA in kidneys. Consistent with the parent PUFA levels, the AA-and DHA-derived lipoxygenase (LOX), cytochrome P450, and nonenzymatic degradation (NE) metabolites increased in kidneys with HFD, while EPA-derived LOX and NE metabolites decreased. Conversely, treatment with AICAR, AMPK activator, reduced the free AA and DHA content and the DHA-derived metabolites in kidney. Interestingly, both kidney and circulating AA, AA metabolites, and EPA-derived LOX and NE metabolites are increased with HFD; whereas, DHA metabolites are increased in kidney in contrast to their decreased circulating levels with HFD. Together, these changes showcase HFD-induced pro- and anti-inflammatory eicosanoid dysregulation and highlight the role of AMPK in correcting HFD-induced dysregulated eicosanoid pathways.

.

INTRODUCTION

The prevalence of obesity has continued to rise over the past few decades and was 36.5% among US adults between the years 2011 to 2014 (1). Obesity serves as a significant risk factor both for the initiation and progression of kidney disease independent of hypertension and diabetes (2-4). Excessive intake of calorie-dense lipids leads to organ dysfunction both by direct lipotoxicity and inflammation. In fact, the western diet enriched in saturated animal fats has been shown to increase albuminuria and cause a faster decline in renal function (5). In our previous studies, we established that HFD induced kidney disease is characterized by renal hypertrophy, increased albuminuria and elevated markers of renal fibrosis and inflammation (6). These HFD-induced markers of inflammation, oxidative stress, and fibrosis are reversed by AMP-activated protein kinase (AMPK) activation (6, 7).

HFD alters the activity of crucial lipid metabolism enzymes Acetyl-CoA carboxylase (ACC) and HMG-CoA reductase (HMGCR) contributing to lipid accumulation in the kidney (6). Total cholesterol esters and phosphatidylcholine content in the kidney are elevated while the fatty acid and triglyceride content is unchanged. Phospholipid accumulation in the proximal tubules is associated with lysosomal dysfunction, stagnant autophagic flux, mitochondrial dysfunction and inflammasome activation (8). High-fat feeding for long periods causes recruitment of macrophages, switch to macrophage pro-inflammatory phenotype and increased inflammatory mediators like TNFα, MCP-1, IL-6, COX-2 and IL-1β (9-12). Diets rich in polyunsaturated fatty acids (PUFAs) are known to change plasma lipids, renal phospholipid content, and subsequently PUFA-derived eicosanoid inflammation in a rat model of nephrotic syndrome (13). However, the influence of renal

eicosanoid synthesis and eicosanoid derived inflammation in HFD induced kidney disease is unknown.

Eicosanoids are oxylipins derived from arachidonic acid (AA) or related PUFAs and are inextricably related to inflammation in the kidney. The primary PUFAs for the *n-6* series and *n-3* series, Linoleic acid (LA) and alpha-linolenic acid (ALA) respectively, are both derived from the diet. These 18-carbon PUFAs are then metabolized by various desaturase and elongase enzymes in a stepwise fashion. However, both LA or ALA are acted on by the same enzymes, resulting in a competition between the *n-3* and *n-6* series (14). LA is metabolized through multiple steps to dihomo-γ-linolenic acid (DGLA, 20:3n6) and, ultimately, to AA (20:4n6). On the other hand, ALA is metabolized to eicosapentaenoic acid (EPA, 20:5 n-3) and subsequently to docosahexaenoic acid (DHA, 22:6 n-3) (15). These PUFAs are incorporated into membrane phospholipids and released by phospholipase A2 (PLA2) under the influence of various stimuli. In subsequent reactions, cyclooxygenases (COX), lipoxygenases (LOX), cytochrome P450 (P450) enzymes act on free PUFAs to form eicosanoids. Some eicosanoids can also be formed from PUFAs via non-enzymatic reactions (NE), e.g., isoprostanes.

Eicosanoids play an essential role in the regulation of renal physiology and disease by modulating renal blood flow, glomerular filtration rate, autoregulation, tubular glomerular feedback, excretion of renal water and sodium, and release of renin and erythropoietin. HFD feeding causes an increase in circulating eicosanoids. In the kidney, these eicosanoids are produced by all different cell types – mesangial cells, renal microvessels, and tubular cells. This makes it difficult to pinpoint the actual origin of these autacoids without actual profiling of the various compartments. Local production in the

kidney will be reflected in the kidney tissue, renal venous compartment, and urine. Recent advances in eicosanoid analysis using highly sensitive mass spectrometry (MS) has enabled us to profile over 150 different eicosanoid metabolites reliably in all tissues, enabling us to systematically profile the changes in the metabolic pathways with HFD and AICAR therapy.

AMPK is a ubiquitous, heterotrimeric kinase that acts as a cellular energy sensor that responds to changes in the intracellular AMP/ATP ratio (16). AICAR (5-aminoimidazole-4-carboxamide-1-β-D-furanosyl 5'-monophosphate) acts as a specific AMPK agonist (17). AMPK activation leads to inhibition of energy-requiring biochemical processes like fatty acid synthesis and stimulation of energy-producing biochemical pathways like beta-oxidation to improve energy efficiency (18). Metabolic stress such as diabetes or obesity impair the activity of AMPK, and AMPK activation reduces the initial and sustained inflammatory response in the kidney of the HFD-induced kidney disease model (6). Along with lipid accumulation, the markers of inflammation were modulated with AICAR use (7). AMPK signaling has been shown to influence the secretory PLA2 expression in vascular smooth muscle cells (19) and control triglyceride content in adipocytes (20). AMPK activation also decreases the formation of 15-LOX metabolites of AA in macrophages (21). While AMPK activation is beneficial in lipid and eicosanoid metabolism in other tissues, the effect of HFD and AMPK activation on eicosanoid pathways in the kidney is unknown. We hypothesized that the high-fat exposure triggers inflammation involving the eicosanoid pathway and that eicosanoid production is ameliorated with AMPK activation. We used a targeted lipidomic platform to systematically investigate the HFD-associated eicosanoid synthesis induced in mice consuming HFD with or without AMPK activation in

order to better understand the pathophysiological processes involved in the HFD-induced kidney disease.

RESULTS

HFD increased phospholipase expression and free levels of polyunsaturated fatty acids and this action is reversed by AMPK activation.

Both cytosolic and secretory PLA2 act on membrane phospholipids to release PUFA's-the precursor of various eicosanoids. Levels of cytosolic phospho-PLA2 (Group IV) and secretory PLA2 were both increased with HFD in the kidney, and AICAR treatment decreased their levels (**Figure 1**).

Targeted lipidomic analysis using MS of kidney tissue revealed unique patterns in the total, and free ω3 and ω6 PUFA series that are demonstrated in **Figure 2.** The total fatty acid (FA) (esterified and unesterified FA) and free FA (unesterified, FFA) profiles generated from the kidney of mice fed a low fat, standard chow (STD), HFD or HFD with the AMPK activator AICAR (HFD+AICAR) are displayed in **Supplemental Table 1**. The total and free EPA are decreased in the kidneys with the HFD (**Figure 2A and B**, $p<0.05$) and further decreased with AICAR, while both total and free DHA, a *n3* fatty acid similar to EPA, is increased with HFD and reversed with the use of AICAR (**Figure 2C and D**, $p<0.05$). While DHA and EPA levels are modulated with HFD, the parent PUFA- ALA (total and unesterified) is unchanged.

Free and total *n6* fatty acid DGLA is decreased in the kidney with HFD but unchanged with AICAR (**Figure 2E and F**). Total and free AA in the kidney are increased

by HFD and the free AA decreased with AICAR (**Figure 2G and H**). Free and total levels of LA, the precursor for both DGLA and AA are unchanged by the diet and AICAR in the kidney. Delta-6 desaturase (D6D) and delta-5 desaturase (D5D) catalyze desaturations at specific positions of FA substrates. Elongases extend the fatty acid carbon chains by two carbons. The levels of both desaturases were not different between the three groups (**Supplementary Figure 1**).

HFD dysregulates kidney eicosanoid metabolism that is ameliorated by AMPK activation.

The eicosanoid metabolites of AA, DHA and EPA are regulated with HFD in the kidney (**Table 1**), and specific metabolites are modulated with AICAR (**Figure 3**). HFD seems to create a clear increase in COX products of AA in the kidney and decrease in COX products of EPA. 12- hydroxyl-hexadecatrienoic acid (12HHT) which is a COX / P450 product is increased with HFD and decreased with AICAR (**Figure 3A**). P450 products of DHA – 16, 17-epoxy-docosapentaenoic acid (16,17-EpDPE) and its product 16-hydroxy-docosahexaenoic acid (16-HDoHE), and 19,20-epoxy-docosapentaenoic acid (19,20-EpDPE) and its product 19,20-dihydroxy-docosapentaenoic acid (19,20-DiHDPA) are increased with HFD, but only the end products 19,20-DiHDPA and 16-HDoHE are decreased with AICAR (**Figure 3B and C**). LOX products of DHA- hydroxy-docosahexaenoic acids (HDoHE): 4-HDoHE, 7-HDoHE, 11-HDoHE, and 17-HDoHE and its product -15 (t)-protectin D1 (15 (t)-PD1) are increased with HFD (**Figure 3D, 3E, and 3F**). NE degradation products of DHA- 8-HDoHE, 10-HDoHE, 13-HDoHE, and 20-HDoHE are increased with HFD and decreased with AICAR (**Figure 3G and 3H**).

HFD and AMPK activation alter the urinary eicosanoid profiles.

HFD induced changes in urine metabolites are illustrated in **Table 2** and the metabolites that are altered with AICAR in **Figure 4**. The overall trend of the kidney continues in the urine with predominant increase of COX products of AA in the urine and decrease of COX products of EPA. Adrenic acid and its COX metabolite dihomo-prostaglandin $PGF_{2\alpha}$ (dihomo-$PGF_{2\alpha}$) are both increased with HFD in the urine but only dihomo-$PGF_{2\alpha}$ is decreased with AICAR (**Figure 4A**). Dihomo-15- deoxyprostaglandin D_2 (dihomo-15d-PGD_2) which is a NE byproduct of another Adrenic acid COX metabolite is decreased with HFD and increased with AICAR (**Figure 4B**).

Urine AA (**Figure 4C**) is increased with HFD and decreased with AICAR which is consistent with the trend in the kidney. Downstream COX metabolites of AA and prostaglandin H_2 (PGH_2) are altered with the HFD and AICAR. P450 metabolite of prostaglandin E_2 (PGE_2) metabolites - 13,14-dihydro-15-keto-prostaglandin E_2 (PGEM, **Figure 4D**) is increased with HFD and decreased with AICAR. Another PGH_2 metabolite-13,14-dihydro-5-keto-prostaglandin $F_{2\alpha}$ (PGFM, **Figure 4E**) and prostaglandin $F_{2\alpha}$ ($PGF_{2\alpha}$, **Figure 4F**) both the products of COX are increased with HFD and decreased with HFD with AICAR. Prostaglandin D_2 (PGD_2) metabolite -prostaglandin J_2 (PGJ_2) is increased with HFD, while urinary 13,14-dihydro-15-keto-prostaglandin D_2 (dhk-PGD_2; **Figure 4G**) both COX metabolites of AA is increased with HFD and decreased with HFD with AICAR following the similar pattern in the kidney AA metabolite 5-iso-prostaglandin $F_{2\alpha}$-VI(5-iso-$PGF_{2\alpha}$-VI) (**Figure 4H**) which is NE product is increased with HFD and decreased with AICAR. Prostaglandin E_3 (PGE_3) is an EPA metabolite of COX action is

increased with HFD and decreased with AICAR (**Figure 4I**). COX metabolites of EPA - Thromboxane B_3 (TXB_3) is decreased with HFD and increased with AICAR (**Figure 4J**).

HFD and AMPK activation modulate circulating eicosanoid levels

In order to delineate the origin of the eicosanoids in the kidney, both the renal artery (**Table 3**) and vein (**Table 4**) were sampled after the mice were fed STD, HFD, and HFD with AICAR. The eicosanoid profile of the arterial and venous samples revealed that AA and its metabolites- 8,9, epoxy-eicosatrienoic acid (8,9 EET) -a product of P450 were both increased with HFD. 5,6- EET and 11,12-EET are increased in the venous circulation but not in the arterial circulation. Since these metabolites are also elevated in the kidney, this suggested the possible production of the metabolites in the kidney and released into the venous circulation. AA COX metabolite 6-keto-prostaglandin $F_{1\alpha}$ is elevated in the venous circulation with HFD – this is in line with the elevation of the downstream metabolite 6-keto-prostaglandin E_1 in the urine.

DHA metabolites- 20-HDoHE, 10-HDoHE, and 13-HDoHE -products of NE degradation are all decreased in the venous circulation. 11-hydroxy-docosahexaenoic acid (11-HDoHE) and 4-HDoHE -products of the LOX pathway while 16-HDoHE the product of P450 are all decreased with HFD in the venous circulation. 4-HDoHE and 20-HDoHE are also decreased with HFD in the arterial circulation.

EPA levels are decreased in both the arterial and venous circulation. EPA produces hydroxy-eicosapentaenoic acid's (HEPE) –NE products,18-HEPE, 11-HEPE, and 9-HEPE were decreased in the arterial and venous circulation. 5-HEPE, 12-HEPE, and 15-HEPE are produced from their respective LOXs and were decreased with HFD in both

the arterial and venous circulation. 15-HEPE is decreased further with AICAR therapy in the arterial circulation. P450 metabolite-14(15)-epoxy-eicosatetraenoic acid (14(15)-EpETE) is decreased with HFD diet in both arterial and venous circulation and further with AICAR in the arterial circulation.

LA metabolites of P450 -9,10-dihydroxy-octadecaenoic acid (9,10-diHOME), 12,13-dihydroxy-octadecaenoic acid (12,13-diHOME), and 12,13-epoxy-octadecaenoic acid (12,13-EpOME) are decreased with HFD and are increased with AICAR in the arterial circulation (**Figure 5A-C**). Venous sampling revealed that 9-hydroxy-octatrienoic acid (9-HOTrE) is a product of LOX derived from ALA is decreased with HFD but increased with AICAR (**Figure 5D**). 5-HEPE is LOX metabolites of EPA is decreased with HFD and increased with AICAR treatment (**Figure 5E**).

Specific eicosanoids are altered by AMPK activation

When taken as a whole, there were significant changes in eicosanoid pathways in arterial and venous circulation, urine and kidney compartments (**Supplementary Table 2**). **Figure 6** depicts the changes influenced by AICAR therapy on HFD mice. To further detect trends in the changes, the highly correlated eicosanoids derived from a parent PUFA and acted on by a specific enzymatic pathways were collapsed in to principal components and analyzed for trends and statistical significance. **Table 5** represents the trends in the kidney and urine of these highly correlated metabolites. In the kidney, HFD decreased EPA metabolites across all enzymatic pathways, while the COX metabolites alone were reversed by AICAR. Meanwhile AA metabolites of urine were mostly elevated with HFD, whereas the COX EPA metabolites are decreased with HFD and this is

reversed with AICAR therapy. COX metabolites of Adrenic acid are decreased with HFD in the urine and this was reversed with AICAR. **Table 6** reveals that EPA, DHA and ALA metabolites were all decreased with HFD in the arterial and venous blood.

DISCUSSION

This is the first study to systematically explore the effects of HFD on eicosanoid synthesis in the kidney and the role of AMPK activation in ameliorating these changes. We find that HFD increases phospholipase A2 expression and activity (through phosphorylation) in the kidney that is largely corrected by AMPK activation. HFD increases both the pro-inflammatory AA and the anti-inflammatory DHA, and their respective downstream products in the kidney and urine and these changes are reversed with AICAR therapy. However, HFD decreases EPA, DGLA, and LOX and NE metabolites of EPA, while AICAR therapy decreases free EPA levels further in the kidney. P450 and NE of LA were decreased in the arterial circulation with HFD are returned to pre-HFD levels with AICAR. These changes highlight the changes in eicosanoid pathways in the kidney with HFD that are ameliorated by AICAR therapy.

Obesity and metabolic syndrome patients have demonstrated altered fatty acid and eicosanoid metabolism compared to lean subjects. Increased serum DGLA levels and low delta-5 desaturase activity was associated with hepatic steatosis over and above conventional risk factors in metabolic syndrome subjects (22). Like our HFD mouse model, COX, LOX, and P450 metabolites of AA and other PUFA's are elevated in the plasma of obese subjects compared to lean subjects (23). Increased TXA_2 can cause vasoconstriction and induce transcription of collagen in the glomerular matrix. In contrast,

PGI_2 counteracts the deleterious TXA_2 effects associated with progressive glomerular damage by acting as a vasodilator. Decreased urinary PGI_2/TXA_2 ratio has been demonstrated in diabetic humans compared to controls (24). In the Japanese population, urinary 8- iso-$PGF_{2\alpha}$ which is a AA metabolite predicts metabolic risks like obesity, hypertension, and glucose tolerance (25). Meanwhile, low serum lipoxin A4 levels (AA metabolite) are associated with metabolic syndrome risk in Chinese population, similar to the elevated kidney levels of lipoxin A4 and its metabolite in our study (26).

Obesity-induced kidney disease is characterized by glomerular enlargement, podocytes loss, and proteinuria eventually leading renal failure (2, 27, 28). In animal models, HFD increased kidney weight and glomerular area with Periodic –Acid-Schiff (PAS) positive matrix and increased Oil red-O positive vacuolated cells. HFD also caused albuminuria, increased glomerular inflammation via the NFκB pathway and increased urinary monocyte chemoattractant protein (MCP-1) and hydrogen peroxide (6, 29). Increased fat intake increases kidney triglyceride content via increased sterol regulatory element proteins -1 and 2 and lipogenesis along with reduced AMPK and increased ACC expression and activity in mice (30) (7, 10). Also, HFD decreased renal lipolysis along with decreased carnitine palmitoyl acyl-CoA transferase-1 expression (31). Mice fed with western diet demonstrated vacuolization of the proximal tubule enriched with multi-lamellar lysosomal bodies with phospholipids the phenomenon was confirmed with human biopsies (32). Human studies have described the accumulation of ectopic lipid in obesity-induced kidney disease (4, 33). Mice lacking the innate immune receptor Nlrp3 did not develop the pathological markers of HFD induced kidney disease indicating

pathways regulated by Nlrp3 could control the development of HFD induced renal pathology (34). Clearly, HFD causes dysregulation of mainstream lipid metabolism in the kidney, but the gateway for many inflammatory mediator's eicosanoid generation with HFD has not been clearly examined.

"The first and rate-limiting step of eicosanoid synthesis is the liberation of PUFAs from their esterified form in the sn-2 position of membrane phospholipids by cytosolic phospholipase. In our study, both the cytosolic (Group IV) and secretory phospholipase A2 were elevated with HFD and decreased with AICAR. Cytosolic PLA2 is essential for adipocyte differentiation in obesity models (35). Cytosolic PLA2 (Group IV) deficient mice are resistant to the hepatic effects of high-fat diet due to the decrease in the production of downstream products confirming the crucial role of this enzyme in high induced fat disease (36). Cytosolic PLA2 is also central to oxidative signaling in renal epithelial cells releasing arachidonic acids and its downstream products (37). Isoenzymes of phospholipase A2 are differentially expressed in various tissues in response to inflammation; for example, expression of group VII phospholipase A2 gene is increased in livers of Zucker obese rats, while expression of group IVA and VIA phospholipase A2 was inhibited (38). Phospholipase A2 isoenzymes also demonstrate substrate selectivity to certain forms of phospholipids in membranes and specific PUFA's (39). Kidney desaturases and elongases that are responsible for conversion between the various PUFA's are unaffected by HFD or AMPK activation in our study. However, livers of obese Zucker rats demonstrated increased expression of delta-6 desaturase and elongase-6 (38). Diets in the HFD and STD groups had similar *n6* to *n3* ratios, and the pattern in the

circulation and the kidney do not reflect this ratio. AA is increased in the circulation, kidney, and urine with HFD in our study and this is consistent with increased circulating PUFA's demonstrated with HFD feeding in Sprague-Dawley rats (40). In excess nutrient states, phospholipase D suppresses AMPK activity through the mammalian/mechanistic target of rapamycin (mTOR); in return, AMPK activation decreased phospholipase D activity similar to the effect of AMPK activation on other phospholipases in vascular smooth muscles, and endothelial cells (19, 41, 42). Thus, the effect of AMPK activation on phospholipases in our study could be responsible for the changes to the PUFA levels with AICAR therapy.

Both COX-1 and COX-2 and their downstream products PGD_2, PGE_2, and PGI_2 are involved in renal vasodilation. PGE_2 is the central prostaglandin synthesized in the kidney tubules and mesangial cells- and activation of its receptors cause contraction of vascular muscle cells, increased calcium in mesangial cells and inhibits sodium reabsorption at the thick ascending limb of the loop of Henle (43). In our study, PGE_2 is decreased in the kidney with HFD, but its metabolites- PGA_2, PGB_2, and PGEM are increased in the urine with HFD. PGI_2 metabolites- 6,15 dk-, dh- $PGF_{1\alpha}$ and 6k-PGE_1 are increased in the urine with HFD similar to PGD_2 metabolites – PGJ_2 and dhkPGD_2. Urinary AA-derived eicosanoids, primarily downstream of COX metabolite-PGH_2 were increased with HFD and decreased with AICAR therapy. Increased flux in these pathways possibly results in decreased bioavailability of the renal vasodilators. In line with our findings, COX-2 expression was increased in renal cortex, blood vessels and in the urine in obese Zucker rats (44). Increased urinary thromboxane B_2 (TXB_2) and 6-keto $PGF_{1\alpha}$ and

decreased PGE_2 excretion rates were evident in obese Zucker rats. Similarly, decreased urinary PGI_2/TXA_2 ratio has been demonstrated in diabetic humans as well as in diabetic animal models. Rofecoxib, a COX-2 inhibitor, decreases vascular and glomerular damage when administered to obese Zucker rats (24). Decreased $PGF_{2\alpha}$ and 8- iso-$PGF_{2\alpha}$ levels contribute to the decreased glomerulosclerosis in obese Zucker rats treated with rofecoxib. COX-2 inhibition and decreases in 8- iso-$PGF_{2\alpha}$ levels have also been shown to ameliorate renal injury associated with hypertensive rats (45). This pattern is also reflected in the urinary levels of 8- iso-$PGF_{2\alpha}$ in our mouse model of HFD induced kidney disease.

Renal P450 epoxidation generates epoxyeicosatrienoic acids (EETs) that are metabolized by soluble epoxide hydrolase (sEH) to less active dihydroxyeicosatrienoic acids (DHETEs). Decreased renal expression of CYP2C epoxygenase enzymes has been observed in diabetes, high fat diet fed insulin resistance rats, and the kidney and mesenteric blood vessels of obese Zucker rats (46). Additionally, sEH expression is increased in blood vessels of obese rats and could further contribute to the decrease in EET bioavailability implicating impaired endothelial dilator responses in obesity and diabetes. Cytokines- IL-6 and TNF-α decrease expression of P450 epoxygenase enzymes. TNF-α and EET's act via NFκB pathway causing elevated MCP-1 levels that have been observed in HFD induced kidney disease in mice (6). Obese Zucker rats have increased renal vascular CYP4A expression and increased generation of 20-HETE (47). However, renal tubular CYP4A expression was decreased in Sprague-Dawley rats on HFD (48). AA metabolites -20-HETE, EET, and DHETE are decreased with HFD in the

kidney and associated with the diet-induced change in blood pressure and renal function of Sprague-Dawley rats (48, 49). In our study, the kidney P450 products of AA- 9-HETE and EET's are increased with HFD just as many of the EET's are also increased in the circulation and urine. Pharmacological inhibition or transgenic deletion of sEH, the dominant enzyme in degrading EETs, have been shown to protect mice from various adverse effects induced by obesity (50). Thus, protective eicosanoid metabolites of AA-EET are increased with HFD in the kidney. In HFD fed mice, plasma profiling revealed increases in circulating P450 metabolite of LA-EpOME's (51) which is a different trend to the one observed in the arterial circulation of our HFD mice maintained on HFD for a longer period.

Central adipose tissue in obese Zucker rats shows increased LOX expression along with inflammatory markers (52). 5-LOX products induce NF-kappaB expression and secretion of inflammatory cytokines like MCP-1, TNF-α, macrophage inflammatory protein-1gamma, and IL-6 by the adipose tissue. The 5-LOX pathway plays a major role in obesity-induced fatty liver disease (53). In our study, LOX metabolites of AA, AA metabolites- 6(R),15 (R)-LXA_4 and 6(S)-LXA_4 are increased in the kidney with HFD in our study, and LXA_4 has been shown by our group to attenuate inflammation in HFD related kidney disease (10). Similarly, LOX metabolites of DHA – HDoHE were elevated in the kidney, whereas LOX metabolites of EPA –HEPE's were all decreased in the kidney and the circulation.

Omega 3 fatty acids – DHA and EPA supplementation in ob/ob mice induced AMPK phosphorylation and alleviated hepatic steatosis. Omega 3 supplementation is

anti-inflammatory, promotes insulin sensitivity and raises *n3* fatty acid-derived resolvins and protectins (54). Obesity significantly decreased DHA-derived 17-hydroxydocosahexaenoic acid (17-HDHA, resolvin D1 precursor) and protectin D1 (PD1) levels in murine adipose tissue. Notably, 17-HDHA treatment reduced adipose tissue expression of inflammatory cytokines, increased adiponectin expression, and improved glucose tolerance parallel to insulin sensitivity in obese mice (55). A concentrated formulation of *n3* PUFAs attenuates albuminuria, renal function, SREBP-1 expression and triglyceride levels in the kidney of type 2 diabetic obese db/db mice (56). DHA and DHA metabolites in the kidney, the various HDoHE's, EpDPE and DiHDPA produced by P450, LOX and NE in the kidney are all increased with HFD in our study. While the kidney and urine DHA metabolites were increased, the circulatory DHA metabolites were decreased- suggesting local production in the kidney. With HFD exposure, DHA metabolites -15 (t)- PD_1 and PDX are both increased in the kidney and urine respectively. In our study, *n3* EPA metabolites – HEPE's were all decreased in the kidney, urine, and circulation. EPA metabolites - PGH_3 and its hydroxyl metabolites were all decreased in the circulation with HFD. Downregulation of HEPE's in our study represents suppression of anti-inflammatory signals.

AMPK is a nutrient sensor and is inhibited by nutrient excess states. In our prior studies, the effects of HFD induced kidney disease were reversed with AMPK activation with AICAR therapy. AMPK activation reversed the inflammatory profile, lipid accumulation, and low adiponectin levels that were caused by HFD (9, 10, 57). Diet reversal alone was unable to improve the renal inflammation and apoptosis in HFD induced kidney damage, emphasizing the persistence of renal injury even after eight

weeks of dietary control (58). However, AMPK activation with metformin treatment was able to reduce the levels of inflammatory and apoptotic markers that remain residual despite diet reversal. Also, metformin ameliorated HFD induced glomerular injury, renal fatty acid oxidation, and serum adipokine levels (58-60). Metformin reduces fat content by decreasing sterol regulatory element-binding protein 1 (SREBP-1), fatty acid synthase (FAS), and acetyl-CoA carboxylase (ACC) expression in the kidney (61). In our study, AICAR reversed the upregulation of phospholipase and free PUFA's. The influence of AICAR is evident in reversing the increased hydroxyl DHA metabolites in the kidney and COX metabolites of AA in the urine. In the venous circulation, AICAR reverses the downregulation of P450 metabolite of LA- 9-HOTrE and LOX metabolite of LA- 5-HEPE. HFD has been previously shown to increase leukotoxins- EpOME, while in our study, EpOME metabolites are decreased (51). AICAR also reverses the downregulation of 9,10 DiHOME, 12, 13-DiHOME, and 12,13-EpOME in the arterial circulation in our study. Thus, AMPK activation is able to reverse key pathways in eicosanoid metabolism and helps ameliorate changes resulting from HFD.

In this current study, we demonstrate modulation of PUFA's and their metabolites after HFD as well as AMPK activation in the kidney, but we cannot delineate the origin of the various eicosanoids in the circulation and urine which could be from the diet, liver, muscle, pancreas and/or gut microbiota. Again, the changes in the eicosanoids might be influenced by the upstream action of phospholipases on specific PUFA's whose pattern might be reflective of the specific diet; Although both the diets had a similar n6: n3 ratio, the specific composition of HFD might have influenced the eicosanoid changes. Also, as the influence of AICAR is not restricted to one specific oxygenase or PUFA, its influence

on phospholipases might influence its action to follow the pattern of the predominant PUFA availability in various compartments. Though we have independently demonstrated the effects of HFD on the kidney pathology, lipid, and inflammatory profile, we cannot conclusively provide evidence that the eicosanoid changes are the sole cause of the HFD induced kidney disease or the reason for the AICAR induced amelioration. Also t eicosanoids might have differential changes based on temporal exposure to HFD, and this was not conclusively studied in our study. It is also difficult to tease out the source of inflammation in such models as both HFD and AICAR therapy, in addition to altering inflammation also influence body weight. Other factor to account for is that pharmacologic AMPK inhibition might not be complete, and genetic manipulation of AMPK might provide a clearer picture. Genetic manipulation of the pathways clearly influenced by AMPK will help us study downstream and upstream changes and their interaction with the eicosanoid pathways and link them to renal pathology.

In summary, in this study using a targeted lipidomic approach, we demonstrate the dysregulation of eicosanoid synthesis and metabolism in the kidney with HFD and its amelioration with AMPK activation. Our work sheds light on the mechanism behind HFD related toxicity and the eicosanoid pathways under the control of AMPK activation in the kidney. We also expose the various pro- and anti-inflammatory mechanisms in HFD mediated kidney disease that are altered with AMPK activation. Future studies manipulating these dysregulated pathways might open therapeutic avenues in the management of high fat induced kidney disease.

CONCISE METHODS

Animals. All animal procedures were approved by the Institutional Animal Care and Use Committee of University of California, San Diego. Male six week old C57BL/6 mice were purchased from Jackson Laboratory (Bar Harbor, ME) were fed a standard diet or a high-fat diet (STD - 5% fat(PUFA 2.1%; *n6* 1.9%; *n3* 0.2%), 24.5% protein, 40% carbohydrate) [HFD - 60% of total calories from fat (90% lard + 10% soybean oil, PUFA 16.9%; *n6* 15.1%; *n3* 1.7%), 20% protein, 20% carbohydrate] (D12492, Research Diets, New Brunswick, NJ) for 14 weeks. The mice on the STD diet were treated with phosphate buffered solution (PBS) and mice on HFD were treated with 5-Aminoimidazole-4-carboxamide-1-β-D-ribofuranoside (AICAR, 0.5 mg/g body weight, Toronto Chemicals) or PBS via intraperitoneal injections for five days a week for a total of 14 weeks (6). Mice were placed in metabolic cages for 24-h urine collection before the start of the diets and after 14 weeks. Mice were sacrificed after 14 weeks of diet plasma was collected from the renal vein, and arterial blood was obtained from direct cardiac puncture. After perfusion with PBS, kidneys were snap-frozen in liquid nitrogen for further analysis.

Quantitative total and free fatty acids analysis: Total and free fatty acids were analyzed by gas chromatography/mass spectrometry (GC-MS) as previously described (62, 63). Briefly, kidney tissue (~10 mg of tissue) was homogenized in 1 mL of PBS containing 10% methanol. For the analysis of total (esterified and free) fatty acids, kidney homogenates (50µL) were spiked with deuterium-labeled fatty acids, acidified with 200 µL of 0.1 N hydrochloric acid and extracted with 500 µL methanol. Phase separation was achieved by the addition of 500 µL of dichloromethane (CH_2Cl_2), and the organic phase

was removed. The extraction with dichloromethane was repeated, and the combined extracts were dried under argon gas. For saponification, the dried lipids were resuspended in 250 µL methanol and 250 µL 4N potassium hydroxide, vortexed for 30 sec and incubated at 37°C for 1 hr. The lipid hydrolysates were then neutralized with 260 µL 4N HCl and the free fatty acids were extracted twice with 2 mL isooctane and the combined extracts containing the hydrolyzed fatty acids were dried under argon before analysis with GC/MS.

Free fatty acids were extracted from 50 µL of the kidney tissue homogenates that was supplemented with a set of deuterated fatty acids that served as internal standards. The extraction was initiated by the addition of 25 µL 1N hydrochloric acid, and 500 µL methanol and a bi-phasic solution were formed by the addition of 1 mL isooctane. The isooctane phase containing the free fatty acid fraction is removed, the extraction is repeated once more, and the combined extracts are dried under argon before analysis with the GC/MS.

In preparation for GC-MS analysis, the fatty acids- both total fatty acid after saponification and free fatty acid extracted from samples and the quantitative standards were taken up in 25 µL of 1% diisopropylethylamine in acetonitrile and derivatized with 25 µL 1% pentafluorobenzyl bromide. The fatty acid esters were analyzed on an Agilent 6890N gas chromatograph equipped with an Agilent 5973 mass selective detector (Agilent, Santa Clara, CA) operated in the negative chemical ionization mode. Fatty acid quantitation was achieved by the stable isotope dilution method.

Quantitative eicosanoid analysis: Eicosanoids were analyzed by liquid chromatography-MS (LC-MS), as described before (63, 64). For tissue analysis, eicosanoids were isolated from 0.9 mL of kidney homogenate supplemented with a set of internal standards consisting of 26 deuterated eicosanoids (Cayman Chemical) by solid phase extraction (Strata-X, Phenomenex, Torrance, CA) and eluted into 1 mL methanol. For eicosanoid analysis in urine, 600 µL of sample were processed identically. The extracted samples were evaporated, reconstituted in 100 µL and a 40 µL aliquot was separated by reverse phase liquid chromatography (LC) using a Synergy C18 column (2.1 x 250 mm, 4 µm; Phenomenex, Torrance, CA). Eicosanoids were analyzed using a tandem quadrupole mass spectrometer (MDS SCIEX 4000 Q Trap; Applied Biosystems, Foster City, CA) via scheduled multiple-reaction monitoring (MRM) in the negative ionization mode. Eicosanoids were identified in samples by matching the MRM signal and LC retention times with those of pure standards. Data analysis was performed using MultiQuant 2.1 software (Applied Biosystems). Quantitative eicosanoid determination was performed using the stable isotope dilution method.

Immunoblot. Kidney tissue homogenates were electrophoretically separated on NuPAGE bis-Tris gels (Life Technologies, USA) and transferred onto nitrocellulose membrane (Life Technologies, USA). Antibodies to ELOLV5, cytosolic phospho-phospholipase A2 and secretory phospholipase 2 (Abcam, USA), FADS1/FADS2 (Biorbyt, UK) and actin (Sigma, USA) were used on the blots. Detection was performed with ECL Plus detection reagents (GE Healthcare, USA) after treatment with appropriate secondary antibody treatment.

Statistical analysis. Results are presented as mean values ± standard deviation. The kidney values were normalized with tissue weight and plasma were normalized to volume. Urinary metabolites are all normalized to urine creatinine values. All metabolites were log transformed and auto-scaled before undergoing statistical analysis using the MetaboAnalyst version 3.0 software, Canada (65). Figures were generated using Graph Pad Prism Software version 4.03, California, USA. Difference between data groups was evaluated for significance using two-way ANOVA and Fisher's least significant difference method (Fisher's LSD) post-hoc tests for multiple comparisons. A p-value less than 0.05 was defined as statistically significant in the non-mass spectrometry experiments. To account for multiple comparisons with a large number of lipid metabolites, false discovery rate (FDR, q value) of <0.05 was considered statistically significant. The highly correlated metabolites were reduced based on eicosanoids derived from a single enzyme pathway from specific parent fatty acid in each tissue compartment were separately aggregated into one secondary variable representative of the corresponding pathway using principal component (PC) analysis. We have then used the PC explaining the highest variance in the variable for further analysis to detect trends using SPSS Version 25, IBM corp (66).

ACKNOWLEDGMENTS

The authors would like to acknowledge the support of grants from the Back to Belgium Grant from the Belgian Federal Science Policy (AED, BELSPO, Belgium); NHLBI K08HL130944 (AVM); DK082841 (KS), DP3DK094532 award (KS); R01DK105961(EAD); and P30DK063491 (EAD, OQ); NIGMS R01GM20501(EAD).

COMPETING INTERESTS

Nothing to declare

AUTHOR CONTRIBUTION

All authors have approved the final manuscript. Among the authors, AED and KS have conceived the experiments; AMA, OQ, and AED have performed the experiments; SP, ED, OQ, and KS have overseen the experiments which were performed in their respective laboratories; AVM and AED conducted all statistical analysis; KS, AVM, and AED have prepared the manuscript.

REFERENCES

1. Ogden, C. L., M. D. Carroll, C. D. Fryar, and K. M. Flegal. 2015. Prevalence of Obesity Among Adults and Youth: United States, 2011-2014. *NCHS data brief*: 1-8.
2. Mathew, A. V., S. Okada, and K. Sharma. 2011. Obesity related kidney disease. *Curr Diabetes Rev* **7**: 41-49.
3. Bruce, K. D., and C. D. Byrne. 2009. The metabolic syndrome: common origins of a multifactorial disorder. *Postgraduate medical journal* **85**: 614-621.
4. de Vries, A. P., P. Ruggenenti, X. Z. Ruan, M. Praga, J. M. Cruzado, I. M. Bajema, V. D. D'Agati, H. J. Lamb, D. Pongrac Barlovic, R. Hojs, M. Abbate, R. Rodriquez, C. E. Mogensen, and E. Porrini. 2014. Fatty kidney: emerging role of ectopic lipid in obesity-related renal disease. *Lancet Diabetes Endocrinol* **2**: 417-426.
5. Lin, J., T. T. Fung, F. B. Hu, and G. C. Curhan. 2011. Association of dietary patterns with albuminuria and kidney function decline in older white women: a subgroup analysis from the Nurses' Health Study. *Am J Kidney Dis* **57**: 245-254.
6. Decleves, A. E., A. V. Mathew, R. Cunard, and K. Sharma. 2011. AMPK mediates the initiation of kidney disease induced by a high-fat diet. *Journal of the American Society of Nephrology : JASN* **22**: 1846-1855.

7. Decleves, A. E., Z. Zolkipli, J. Satriano, L. Wang, T. Nakayama, M. Rogac, T. P. Le, J. L. Nortier, M. G. Farquhar, R. K. Naviaux, and K. Sharma. 2014. Regulation of lipid accumulation by AMK-activated kinase in high fat diet-induced kidney injury. *Kidney Int* **85**: 611-623.
8. Yamamoto, T., Y. Takabatake, A. Takahashi, T. Kimura, T. Namba, J. Matsuda, S. Minami, J. Y. Kaimori, I. Matsui, T. Matsusaka, F. Niimura, M. Yanagita, and Y. Isaka. 2017. High-Fat Diet-Induced Lysosomal Dysfunction and Impaired Autophagic Flux Contribute to Lipotoxicity in the Kidney. *J Am Soc Nephrol* **28**: 1534-1551.
9. Borgeson, E., V. Wallenius, G. H. Syed, M. Darshi, J. Lantero Rodriguez, C. Biorserud, M. Ragnmark Ek, P. Bjorklund, M. Quiding-Jarbrink, L. Fandriks, C. Godson, and K. Sharma. 2017. AICAR ameliorates high-fat diet-associated pathophysiology in mouse and ex vivo models, independent of adiponectin. *Diabetologia* **60**: 729-739.
10. Börgeson, E., A. M. F. Johnson, Y. S. Lee, A. Till, G. H. Syed, S. T. Ali-Shah, P. J. Guiry, J. Dalli, R. A. Colas, C. N. Serhan, K. Sharma, and C. Godson. 2015. Lipoxin A(4) attenuates obesity-induced adipose inflammation and associated liver and kidney disease. *Cell metabolism* **22**: 125-137.
11. van der Heijden, R. A., J. Bijzet, W. C. Meijers, G. K. Yakala, R. Kleemann, T. Q. Nguyen, R. A. de Boer, C. G. Schalkwijk, B. P. C. Hazenberg, U. J. F. Tietge, and P. Heeringa. 2015. Obesity-induced chronic inflammation in high fat diet challenged C57BL/6J mice is associated with acceleration of age-dependent renal amyloidosis. *Scientific reports* **5**: 16474.
12. Altunkaynak, M. E., E. Özbek, B. Z. Altunkaynak, İ. Can, D. Unal, and B. Unal. 2008. The effects of high-fat diet on the renal structure and morphometric parametric of kidneys in rats. *Journal of Anatomy* **212**: 845-852.
13. Barcelli, U. O., D. C. Beach, B. Thompson, M. Weiss, and V. E. Pollak. 1988. A diet containing n−3 and n−6 fatty acids favorably alters the renal phospholipids, eicosanoid synthesis and plasma lipids in nephrotic rats. *Lipids* **23**: 1059-1063.
14. Nakamura, M. T., and T. Y. Nara. 2003. Essential fatty acid synthesis and its regulation in mammals. *Prostaglandins, leukotrienes, and essential fatty acids* **68**: 145-150.
15. Schmitz, G., and J. Ecker. 2008. The opposing effects of n-3 and n-6 fatty acids. *Prog Lipid Res* **47**: 147-155.
16. Carling, D. 2004. The AMP-activated protein kinase cascade--a unifying system for energy control. *Trends in biochemical sciences* **29**: 18-24.
17. Corton, J. M., J. G. Gillespie, S. A. Hawley, and D. G. Hardie. 1995. 5-aminoimidazole-4-carboxamide ribonucleoside. A specific method for activating AMP-activated protein kinase in intact cells? *Eur J Biochem* **229**: 558-565.
18. Hardie, D. G., S. A. Hawley, and J. W. Scott. 2006. AMP-activated protein kinase--development of the energy sensor concept. *J Physiol* **574**: 7-15.
19. El Hadri, K., C. Denoyelle, L. Ravaux, B. Viollet, M. Foretz, B. Friguet, M. Rouis, and M. Raymondjean. 2015. AMPK Signaling Involvement for the Repression of the IL-1β-Induced Group IIA Secretory Phospholipase A2 Expression in VSMCs. *PLOS ONE* **10**: e0132498.
20. Jiang, S., H. Chen, Z. Wang, J. J. Riethoven, Y. Xia, J. Miner, and M. Fromm. 2011. Activated AMPK and prostaglandins are involved in the response to conjugated

linoleic acid and are sufficient to cause lipid reductions in adipocytes. *The Journal of nutritional biochemistry* **22**: 656-664.
21. Namgaladze, D., R. G. Snodgrass, C. Angioni, N. Grossmann, N. Dehne, G. Geisslinger, and B. Brüne. 2015. AMP-activated Protein Kinase Suppresses Arachidonate 15-Lipoxygenase Expression in Interleukin 4-polarized Human Macrophages. *Journal of Biological Chemistry* **290**: 24484-24494.
22. Matsuda, M., T. Kawamoto, and R. Tamura. 2017. Predictive value of serum dihomo-gamma-linolenic acid level and estimated Delta-5 desaturase activity in patients with hepatic steatosis. *Obes Res Clin Pract* **11**: 34-43.
23. Li, S., Q. Chu, J. Ma, Y. Sun, T. Tao, R. Huang, Y. Liao, J. Yue, J. Zheng, L. Wang, X. Xue, M. Zhu, X. Kang, H. Yin, and W. Liu. 2017. Discovery of Novel Lipid Profiles in PCOS: Do Insulin and Androgen Oppositely Regulate Bioactive Lipid Production? *J Clin Endocrinol Metab* **102**: 810-821.
24. Dey, A., C. Maric, W. H. Kaesemeyer, C. Z. Zaharis, J. Stewart, J. S. Pollock, and J. D. Imig. 2004. Rofecoxib decreases renal injury in obese Zucker rats. *Clin Sci (Lond)* **107**: 561-570.
25. Mure, K., N. Yoshimura, M. Hashimoto, S. Muraki, H. Oka, S. Tanaka, H. Kawaguchi, K. Nakamura, T. Akune, and T. Takeshita. 2015. Urinary 8-iso-prostaglandin F2alpha as a marker of metabolic risks in the general Japanese population: The ROAD study. *Obesity (Silver Spring)* **23**: 1517-1524.
26. Yu, D., Z. Xu, X. Yin, F. Zheng, X. Lin, Q. Pan, and H. Li. 2015. Inverse Relationship between Serum Lipoxin A4 Level and the Risk of Metabolic Syndrome in a Middle-Aged Chinese Population. *PLoS One* **10**: e0142848.
27. Chen, H. M., Z. H. Liu, C. H. Zeng, S. J. Li, Q. W. Wang, and L. S. Li. 2006. Podocyte lesions in patients with obesity-related glomerulopathy. *Am J Kidney Dis* **48**: 772-779.
28. Kambham, N., G. S. Markowitz, A. M. Valeri, J. Lin, and V. D. D'Agati. 2001. Obesity-related glomerulopathy: an emerging epidemic. *Kidney Int* **59**: 1498-1509.
29. Mima, A., T. Yasuzawa, G. L. King, and S. Ueshima. 2018. Obesity-associated glomerular inflammation increases albuminuria without renal histological changes. *FEBS open bio* **8**: 664-670.
30. Jiang, T., Z. Wang, G. Proctor, S. Moskowitz, S. E. Liebman, T. Rogers, M. S. Lucia, J. Li, and M. Levi. 2005. Diet-induced obesity in C57BL/6J mice causes increased renal lipid accumulation and glomerulosclerosis via a sterol regulatory element-binding protein-1c-dependent pathway. *The Journal of biological chemistry* **280**: 32317-32325.
31. Kume, S., T. Uzu, S. Araki, T. Sugimoto, K. Isshiki, M. Chin-Kanasaki, M. Sakaguchi, N. Kubota, Y. Terauchi, T. Kadowaki, M. Haneda, A. Kashiwagi, and D. Koya. 2007. Role of altered renal lipid metabolism in the development of renal injury induced by a high-fat diet. *Journal of the American Society of Nephrology : JASN* **18**: 2715-2723.
32. Rampanelli, E., P. Ochodnicky, J. P. Vissers, L. M. Butter, N. Claessen, A. Calcagni, L. Kors, L. A. Gethings, S. J. Bakker, M. H. de Borst, G. J. Navis, G. Liebisch, D. Speijer, M. A. van den Bergh Weerman, B. Jung, J. Aten, E. Steenbergen, G. Schmitz, A. Ballabio, S. Florquin, J. M. Aerts, and J. C. Leemans. 2018. Excessive dietary lipid intake provokes an acquired form of lysosomal lipid storage disease in the kidney. *J Pathol* **246**: 470-484.

33. D'Agati, V. D., A. Chagnac, A. P. de Vries, M. Levi, E. Porrini, M. Herman-Edelstein, and M. Praga. 2016. Obesity-related glomerulopathy: clinical and pathologic characteristics and pathogenesis. *Nat Rev Nephrol* **12**: 453-471.
34. Bakker, P. J., L. M. Butter, L. Kors, G. J. Teske, J. Aten, F. S. Sutterwala, S. Florquin, and J. C. Leemans. 2014. Nlrp3 is a key modulator of diet-induced nephropathy and renal cholesterol accumulation. *Kidney Int* **85**: 1112-1122.
35. Pena, L., C. Meana, A. M. Astudillo, G. Lorden, M. Valdearcos, H. Sato, M. Murakami, J. Balsinde, and M. A. Balboa. 2016. Critical role for cytosolic group IVA phospholipase A2 in early adipocyte differentiation and obesity. *Biochim Biophys Acta* **1861**: 1083-1095.
36. Ii, H., N. Yokoyama, S. Yoshida, K. Tsutsumi, S. Hatakeyama, T. Sato, K. Ishihara, and S. Akiba. 2009. Alleviation of high-fat diet-induced fatty liver damage in group IVA phospholipase A2-knockout mice. *PLoS One* **4**: e8089.
37. Cui, X.-L., Y. Ding, L. D. Alexander, C. Bao, O. K. Al-Khalili, M. Simonson, D. C. Eaton, and J. G. Douglas. 2006. Oxidative signaling in renal epithelium: Critical role of cytosolic phospholipase A2 and p38(SAPK). *Free radical biology & medicine* **41**: 213-221.
38. Fevre, C., S. Bellenger, A. S. Pierre, M. Minville, J. Bellenger, J. Gresti, M. Rialland, M. Narce, and C. Tessier. 2011. The metabolic cascade leading to eicosanoid precursors--desaturases, elongases, and phospholipases A2--is altered in Zucker fatty rats. *Biochim Biophys Acta* **1811**: 409-417.
39. Diez, E., F. H. Chilton, G. Stroup, R. J. Mayer, J. D. Winkler, and A. N. Fonteh. 1994. Fatty acid and phospholipid selectivity of different phospholipase A2 enzymes studied by using a mammalian membrane as substrate. *Biochem J* **301 (Pt 3)**: 721-726.
40. Liu, T.-W., T. D. Heden, E. M. Morris, K. L. Fritsche, V. J. Vieira-Potter, and J. P. Thyfault. 2015. High-fat diet alters serum fatty acid profiles in obesity prone rats: implications for in-vitro studies. *Lipids* **50**: 997-1008.
41. Mukhopadhyay, S., M. Saqcena, A. Chatterjee, A. Garcia, M. A. Frias, and D. A. Foster. 2015. Reciprocal regulation of AMP-activated protein kinase and phospholipase D. *The Journal of biological chemistry* **290**: 6986-6993.
42. Yang, L., H.-L. Cong, S.-F. Wang, and T. Liu. 2017. AMP-activated protein kinase mediates the effects of lipoprotein-associated phospholipase A2 on endothelial dysfunction in atherosclerosis. *Experimental and therapeutic medicine* **13**: 1622-1629.
43. Breyer, M. D., Y. Zhang, Y. F. Guan, C. M. Hao, R. L. Hebert, and R. M. Breyer. 1998. Regulation of renal function by prostaglandin E receptors. *Kidney Int Suppl* **67**: S88-94.
44. Dey, A., R. S. Williams, D. M. Pollock, D. W. Stepp, J. W. Newman, B. D. Hammock, and J. D. Imig. 2004. Altered Kidney CYP2C and Cyclooxygenase-2 Levels Are Associated with Obesity-Related Albuminuria. *Obesity Research* **12**: 1278-1289.
45. Tomida, T., Y. Numaguchi, Y. Nishimoto, M. Tsuzuki, Y. Hayashi, H. Imai, H. Matsui, and K. Okumura. 2003. Inhibition of COX-2 prevents hypertension and proteinuria associated with a decrease of 8-iso-PGF2alpha formation in L-NAME-treated rats. *J Hypertens* **21**: 601-609.
46. Zhao, X., A. Dey, O. P. Romanko, D. W. Stepp, M. H. Wang, Y. Zhou, L. Jin, J. S. Pollock, R. C. Webb, and J. D. Imig. 2005. Decreased epoxygenase and increased

epoxide hydrolase expression in the mesenteric artery of obese Zucker rats. *Am J Physiol Regul Integr Comp Physiol* **288**: R188-196.
47. Dey, A., R. S. Williams, D. M. Pollock, D. W. Stepp, J. W. Newman, B. D. Hammock, and J. D. Imig. 2004. Altered kidney CYP2C and cyclooxygenase-2 levels are associated with obesity-related albuminuria. *Obes Res* **12**: 1278-1289.
48. Wang, M. H., A. Smith, Y. Zhou, H. H. Chang, S. Lin, X. Zhao, J. D. Imig, and A. M. Dorrance. 2003. Downregulation of renal CYP-derived eicosanoid synthesis in rats with diet-induced hypertension. *Hypertension* **42**: 594-599.
49. Zhou, Y., S. Lin, H.-H. Chang, J. Du, Z. Dong, A. M. Dorrance, M. W. Brands, and M.-H. Wang. 2005. Gender differences of renal CYP-derived eicosanoid synthesis in rats fed a high-fat diet*. *American Journal of Hypertension* **18**: 530-537.
50. Iyer, A., K. Kauter, M. A. Alam, S. H. Hwang, C. Morisseau, B. D. Hammock, and L. Brown. 2012. Pharmacological inhibition of soluble epoxide hydrolase ameliorates diet-induced metabolic syndrome in rats. *Experimental diabetes research* **2012**: 758614.
51. Wang, W., J. Yang, H. Yang, K. Z. Sanidad, B. D. Hammock, D. Kim, and G. Zhang. 2016. Effects of high-fat diet on plasma profiles of eicosanoid metabolites in mice. *Prostaglandins & Other Lipid Mediators* **127**: 9-13.
52. Chakrabarti, S. K., Y. Wen, A. D. Dobrian, B. K. Cole, Q. Ma, H. Pei, M. D. Williams, M. H. Bevard, G. E. Vandenhoff, S. R. Keller, J. Gu, and J. L. Nadler. 2011. Evidence for activation of inflammatory lipoxygenase pathways in visceral adipose tissue of obese Zucker rats. *Am J Physiol Endocrinol Metab* **300**: E175-187.
53. Martinez-Clemente, M., J. Claria, and E. Titos. 2011. The 5-lipoxygenase/leukotriene pathway in obesity, insulin resistance, and fatty liver disease. *Current opinion in clinical nutrition and metabolic care* **14**: 347-353.
54. Gonzalez-Periz, A., R. Horrillo, N. Ferre, K. Gronert, B. Dong, E. Moran-Salvador, E. Titos, M. Martinez-Clemente, M. Lopez-Parra, V. Arroyo, and J. Claria. 2009. Obesity-induced insulin resistance and hepatic steatosis are alleviated by omega-3 fatty acids: a role for resolvins and protectins. *Faseb j* **23**: 1946-1957.
55. Neuhofer, A., M. Zeyda, D. Mascher, B. K. Itariu, I. Murano, L. Leitner, E. E. Hochbrugger, P. Fraisl, S. Cinti, C. N. Serhan, and T. M. Stulnig. 2013. Impaired local production of proresolving lipid mediators in obesity and 17-HDHA as a potential treatment for obesity-associated inflammation. *Diabetes* **62**: 1945-1956.
56. Katakura, M., M. Hashimoto, T. Inoue, A. Al Mamun, Y. Tanabe, R. Iwamoto, M. Arita, S. Tsuchikura, and O. Shido. 2014. Omega-3 fatty acids protect renal functions by increasing docosahexaenoic acid-derived metabolite levels in SHR.Cg-Lepr(cp)/NDmcr rats, a metabolic syndrome model. *Molecules* **19**: 3247-3263.
57. Sharma, K., S. Ramachandrarao, G. Qiu, H. K. Usui, Y. Zhu, S. R. Dunn, R. Ouedraogo, K. Hough, P. McCue, L. Chan, B. Falkner, and B. J. Goldstein. 2008. Adiponectin regulates albuminuria and podocyte function in mice. *J Clin Invest* **118**: 1645-1656.
58. Tikoo, K., E. Sharma, V. R. Amara, H. Pamulapati, and V. S. Dhawale. 2016. Metformin Improves Metabolic Memory in High Fat Diet (HFD)-induced Renal Dysfunction. *The Journal of biological chemistry* **291**: 21848-21856.
59. Kim, D., J. E. Lee, Y. J. Jung, A. S. Lee, S. Lee, S. K. Park, S. H. Kim, B. H. Park, W. Kim, and K. P. Kang. 2013. Metformin decreases high-fat diet-induced renal injury by

regulating the expression of adipokines and the renal AMP-activated protein kinase/acetyl-CoA carboxylase pathway in mice. *Int J Mol Med* **32**: 1293-1302.
60. Mount, P., M. Davies, S. W. Choy, N. Cook, and D. Power. 2015. Obesity-Related Chronic Kidney Disease-The Role of Lipid Metabolism. *Metabolites* **5**: 720-732.
61. Wang, W., X. H. Guo, H. H. Wu, N. H. Wang, and X. S. Xu. 2006. [Effect of fenofibrate and metformin on lipotoxicity in OLETF rat kidney]. *Beijing da xue xue bao. Yi xue ban = Journal of Peking University. Health sciences* **38**: 170-175.
62. Quehenberger, O., A. M. Armando, and E. A. Dennis. 2011. High sensitivity quantitative lipidomics analysis of fatty acids in biological samples by gas chromatography-mass spectrometry. *Biochim Biophys Acta* **1811**: 648-656.
63. Quehenberger, O., A. M. Armando, A. H. Brown, S. B. Milne, D. S. Myers, A. H. Merrill, S. Bandyopadhyay, K. N. Jones, S. Kelly, R. L. Shaner, C. M. Sullards, E. Wang, R. C. Murphy, R. M. Barkley, T. J. Leiker, C. R. Raetz, Z. Guan, G. M. Laird, D. A. Six, D. W. Russell, J. G. McDonald, S. Subramaniam, E. Fahy, and E. A. Dennis. 2010. Lipidomics reveals a remarkable diversity of lipids in human plasma. *Journal of lipid research* **51**: 3299-3305.
64. Dumlao, D. S., M. W. Buczynski, P. C. Norris, R. Harkewicz, and E. A. Dennis. 2011. High-throughput lipidomic analysis of fatty acid derived eicosanoids and N-acylethanolamines. *Biochimica et biophysica acta* **1811**: 724-736.
65. Xia, J., and D. S. Wishart. 2002. Using MetaboAnalyst 3.0 for Comprehensive Metabolomics Data Analysis. *In* Current Protocols in Bioinformatics. John Wiley & Sons, Inc.
66. Afshinnia, F., L. Zeng, J. Byun, S. Wernisch, R. Deo, J. Chen, L. Hamm, E. R. Miller, E. P. Rhee, M. J. Fischer, K. Sharma, H. I. Feldman, G. Michailidis, and S. Pennathur. 2018. Elevated lipoxygenase and cytochrome P450 products predict progression of chronic kidney disease. *Nephrol Dial Transplant*.

Table 1: Eicosanoid metabolites altered with high-fat diet in the kidney

Name	Acronym	MECH	STD	HFD	p value	q value
Up with HFD						
Arachidonic acid metabolites						
Arachidonic acid	AA	PUFA	243.4±19.2	312.7±40.9	0.010	0.037
13,14-dihydro-15-keto-prostaglandin D_2	dhk-PGD_2	COX	0.04 ± 0.01	1.20 ± 0.02	0.008	0.035
5,6-epoxy-eicosotrienoic acid	5,6-EET	P450	1.59 ± 0.74	8.64 ± 5.64	0.014	0.045
11,12-epoxy-eicosotrienoic acid	11,12-EET	P450	0.02 ± 0.01	0.18 ± 0.13	0.015	0.045
5-oxo-eicosotetraenoic acid	5-oxoETE	LOX	0.22 ± 0.11	1.56 ± 1.21	0.013	0.043
6(R),15(R)-lipoxin A_4	6(R),15(R)-LXA_4	LOX	0.02 ± 0.01	0.05 ± 0.02	0.006	0.032
6(S)-lipoxin A_4	6SLXA_4	LOX	0.02 ± 0.01	0.05 ± 0.02	0.015	0.045
9-hydroxy-eicosotetraenoic acid	9-HETE	NE	0.02 ± 0.01	0.14 ± 0.09	0.013	0.043
Docosahexaenoic acid metabolites						
16,17-epoxy-docosapentenoic acid	16,17-EpDPE	P450	0.42±0.07	0.65±0.08	0.001	0.010
16-hydroxy-docosahexaenoic acid	16-HDoHE	P450	0.60±0.07	1.20±0.24	<0.001	0.003
19,20-epoxy-docosopentenoic acid	19,20-EpDPE	P450	1.03±0.19	1.63±0.22	0.001	0.010
19,20-dihydroxy-docosapentenoic acid	19,20-DiHDPA	P450	0.55±0.10	1.32±0.43	0.001	0.008
4-hydroxy-docosahexaenoic acid	4-HDoHE	LOX	1.22±0.20	3.17±1.36	0.007	0.032
7-hydroxy-docosahexaenoic acid	7-HDoHE	LOX	0.17±0.02	0.32±0.09	0.004	0.021
11-hydroxy-docosahexaenoic acid	11-HDoHE	LOX	0.25±0.03	0.45±0.06	<0.001	0.001
17-hydroxy-docosahexaenoic acid	17-HDoHE	LOX	1.04±0.13	1.84±0.31	<0.001	0.005
Protectin DX	PDX	LOX	0.02±0.01	0.07±0.02	0.009	0.037
15 (t)-protectin D_1	15(t)-PD_1	LOX	4.14±0.89	12.68±3.76	0.001	0.008
8-hydroxy-docosahexaenoic acid	8-HDoHE	NE	0.67±0.08	1.16±0.24	0.001	0.009
10-hydroxy-docosahexaenoic acid	10-HDoHE	NE	0.26±0.03	0.45±0.07	0.001	0.007
13-hydroxy-docosahexaenoic acid	13-HDoHE	NE	0.51±0.10	0.78±0.11	0.003	0.017
20-hydroxy-docosahexaenoic acid	20-HDoHE	NE	1.61±0.22	2.46±0.40	0.002	0.013
Eicosapentaenoic acid metabolites						
11-hydroxy-eicosapentaenoic acid	11-HEPE	NE	0.28±0.10	2.0±1.50	0.010	0.037
Down with HFD						
Arachidonic acid metabolites						
Prostaglandin E_2	PGE_2	COX	2.88±1.02	1.43±0.21	0.011	0.040
Dihomo-Y-linoleic acid metabolites						
15-keto-Prostaglandin $F_{1\alpha}$	15-ketoP$GF_{1\alpha}$	COX	0.43±0.09	0.23±0.08	0.007	0.032
15-hydroxy-eicosatrienoic acid	15-HETrE	LOX	0.46±0.07	0.34±0.04	0.009	0.037
Eicosapentaenoic acid metabolites						
5-hydroxy-eicosapentaenoic acid	5-HEPE	LOX	0.24±0.03	0.09±0.02	<0.001	0.001
12-hydroxy-eicosapentaenoic acid	12-HEPE	LOX	4.23±0.31	1.17±0.26	<0.001	<0.001
15-hydroxy-eicosapentaenoic acid	15-HEPE	LOX	0.15±0.02	0.05±0.01	<0.001	<0.001
18-hydroxy-eicosapentaenoic acid	18-HEPE	NE	0.22±0.03	0.07±0.01	<0.001	<0.001

MECH- mechanism; STD – standard diet; HFD- high-fat diet; PUFA – polyunsaturated fatty acid; COX –cyclooxygenase; LOX –lipoxygenase; P450-cytochrome P450; NE- non-enzymatic degradation. All values are pmol/ mg renal tissue expressed as mean ± SD

Table 2: Eicosanoid metabolites altered with high-fat diet in the urine

Colun	Name	Acronym	MECH	STD	HFD	p value	q value
Up with HFD							
Adrenic acid metabolites							
	Adrenic acid	Adrenic Acid	PUFA	0.018±0.009	0.27±0.27	0.001	0.011
	Dihomo-prostaglandin $F_{2\alpha}$	dihomo-$PGF_{2\alpha}$	COX	0.009±0.003	0.62±0.18	<0.001	<0.001
Arachidonic acid metabolites							
	Arachidonic acid	AA	PUFA	1.768±0.619	14.7±8.9	<0.001	0.003
	Prostaglandin A_2	PGA_2	COX	0.018±0.018	0.09±0.03	0.001	0.011
	Prostaglandin B_2	PGB_2	COX	0.035±0.009	0.09±0.09	<0.001	0.005
	13,14-dihydro-15- keto- prostaglandin E_2	PGEM	COX	0.354±0.035	1.23±0.17	<0.001	<0.001
	Prostaglandin J_2	PGJ_2	COX	0.002±0.002	0.009±0.004	0.002	0.017
	13,14-dihydro-15-keto-prostaglandin D_2	dhk-PGD_2	COX	0.008±0.003	0.026±0.004	<0.001	<0.001
	6,15-diketo-13,14-dihydro-prostaglandin $F_{1\alpha}$	6,15 dk-,dh- $PGF_{1\alpha}$	COX	0.27±0.09	2.12±0.79	<0.001	0.001
	Prostaglandin $F_{2\alpha}$	$PGF_{2\alpha}$	COX	0.001±0.001	0.09±0.026	0.004	0.023
	13,14-dihydro-15- keto-prostaglandin $F_{2\alpha}$	PGFM	COX	1.59±0.26	7.25±1.76	<0.001	<0.001
	6-keto-prostaglandin E_1	$6kPGE_1$	COX	0.09±0.009	0.09±0.017	0.002	0.013
	8,9-dihydroxy-eicosotrienoic acid	8,9-diHETrE	P450	0.002±0.0009	0.006±0.0017	<0.001	0.001
	11,12-epoxy-eicosatrienoic acid	11,12-EET	P450	0.002±0.0009	0.005±0.002	0.002	0.013
	Eoxin D_4	EXD_4	LOX	20.69±13.26	192.5±69.2	<0.001	0.001
	Eoxin E_4	EXE_4	LOX	0.088±0.088	2.56±1.6	0.009	0.045
	5-iso-prostaglandin $F_{2\alpha}$-VI	5-iso-$PGF_{2\alpha}$-VI	NE	0.026±0.007	0.09±0.09	<0.001	0.001
	8-iso-prostaglandin $F_{2\alpha}$	8-iso-$PGF_{2\alpha}$	NE	0.08±0.009	0.17±0.09	0.008	0.042
Docosahexanoic acid metabolites							
	Protectin DX	PDX	LOX	11.22±13.96	27.5±8.7	0.008	0.042
	19,20-dihydroxy-docosapentenoic acid	19,20-DiHDPA	P450	0.009±0.006	0.026±0.017	0.009	0.046
Eicosopentaenoic acid metabolites							
	Prostaglandin E_3	PGE_3	COX	0.18±0.09	3.62±2.12	<0.001	0.000
Linoleic acid metabolites							
	9-oxo-octadecadienoic acid	9-oxoODE	COX	2.39±0.97	54.7±2.1	0.001	0.011
Down with HFD							
Eicosopentaenoic acid metabolites							
	Prostaglandin D_3	PGD_3	COX	0.71±0.26	0.17±0.17	0.003	0.021
	Prostaglandin $F_{3\alpha}$	$PGF_{3\alpha}$	COX	73739.8±35060.	18813.4±1562	0.001	0.011
	Thromboxane B_3	TXB_3	COX	0.044±0.009	0.026±0.009	0.008	0.042

MECH- mechanism; STD – standard diet; HFD- high-fat diet; PUFA – polyunsaturated fatty acid; COX –cyclooxygenase; LOX –lipoxygenase; P450-cytochrome P450; NE- non-enzymatic degradation. All values are ng per mg creatinine expressed as mean ± SD.

Table 3: Eicosanoid metabolites altered with high-fat diet in the arterial circulation

Column1	Name	Acronym	MECH	STD	HFD	p value	q value
Up with HFD							
Arachidonic acid metabolites							
	Arachidonic acid	AA	PUFA	8771.3±1930.9	14906.2±2726.5	0.002	0.011
	8,9-epoxy-eicosotrienoic acid	8,9-EET	P450	0.10±0.14	3.77±3.41	0.001	0.005
Down with HFD							
Alpha Linoleic acid metabolites							
	9-hydroxy-octatrienoic acid	9-HOTrE	LOX	2.97±0.90	0.99±0.31	<0.001	0.003
Docosahexaenoic acid metabolites							
	4-hydoxy-docosahexaenoic acid	4-HDoHE	LOX	8.93±1.43	3.45±0.91	<0.001	0.001
	11-hydoxy-docosahexaenoic acid	11-HDoHE	LOX	3.03±1.13	1.35±0.80	0.014	0.042
	16-hydoxy-docosahexaenoic acid	16-HDoHE	P450	1.49±0.55	0.58±0.17	0.002	0.012
	10-hydoxy-docosahexaenoic acid	10-HDoHE	NE	2.56±0.92	1.05±0.52	0.009	0.031
	13-hydoxy-docosahexaenoic acid	13-HDoHE	NE	3.62±0.27	1.94±0.81	0.010	0.033
	20-hydoxy-docosahexaenoic acid	20-HDoHE	NE	1.49±0.62	0.11±0.10	0.002	0.011
Eicosapentaenoic acid metabolites							
	Eicosapentaenoic acid	EPA	PUFA	12331.9±4377.1	4870.6±1329.8	0.003	0.011
	5-hydroxy-eicosapentaenoic acid	5-HEPE	LOX	2.53±0.28	0.38±0.13	<0.001	0.003
	12-hydroxy-eicosapentaenoic acid	12-HEPE	LOX	33.76±22.64	4.46±3.22	0.004	0.013
	15-hydroxy-eicosapentaenoic acid	15-HEPE	LOX	1.65±0.45	0.20±0.13	0.004	0.013
	14(15)-epoxy-eicosatetraenoic acid	14,15-EpETE	P450	0.56±0.18	0.18±0.05	<0.001	0.003
	9-hydroxy-eicosapentaenoic acid	9-HEPE	NE	3.56±1.84	0.11±0.13	<0.001	0.003
	11-hydroxy-eicosapentaenoic acid	11-HEPE	NE	1.45±0.18	0.18±0.07	<0.001	<0.001
	18-hydroxy-eicosapentaenoic acid	18-HEPE	NE	1.51±0.26	0.19±0.11	<0.001	<0.001
Linoleic acid metabolites							
	9,10-dihydroxy-octadecaenoic acid	9,10-diHOME	P450	16.71±6.03	7.38±4.10	0.013	0.041
	12,13-epoxy-octadecenoic acid	12,13-EpOME	P450	12.65±3.65	5.52±2.11	0.002	0.012
	12,13-dihydroxy-octadecenoic acid	12,13-diHOME	P450	38.64±13.16	10.86±6.82	0.001	0.005
	13-hydroxy-octadecadienoic acid	13-HODE	NE	61.13±20.15	23.91±8.93	0.005	0.015

MECH- mechanism; STD – standard diet; HFD- high-fat diet; PUFA – polyunsaturated fatty acid; COX –cyclooxygenase; LOX –lipoxygenase; P450-cytochrome P450; NE- non-enzymatic degradation. All values are pmol/ml plasma expressed as mean ± SD.

Table 4: Eicosanoid metabolites altered with high-fat diet in the venous circulation

Column1	Name	Acronym	MECH	STD	HFD	p value	q value
Up with HFD							
Arachidonic acid metabolites							
	Arachidonic acid	AA	PUFA	7763.6±1110.5	13307.3±2881.1	0.001	0.009
	8.9-epoxy-eicosotrienoic acid	8,9-EET	P450	0.04±0.08	0.51±0.41	0.012	0.049
	5,6-epoxy-eicosotrienoic acid	5,6-EET	P450	8.26±4.66	20.49±6.51	0.006	0.031
	11,12-epoxy-eicosotrienoic acid	11,12-EET	P450	1.82±0.65	3.89±0.97	0.002	0.015
	6-keto-prostaglandin F1α	6k-PGF$_{1\alpha}$	COX	1.11±0.44	2.64±1.14	0.005	0.027
Down with HFD							
Docosahexaenoic acid metabolites							
	4-hydroxy-docosahexaenoic acid	4-HDoHE	LOX	9.87±2.09	3.26±0.61	<0.001	0.001
	20-hydroxy-docosahexaenoic acid	20-HDoHE	NE	0.89±0.33	0.13±0.22	0.004	0.027
Alpha Linolenic acid metabolites							
	9-hydroxy-octatrienoic acid	9-HOTrE	LOX	1.87±0.68	0.69±0.21	0.001	0.007
Eicosapentaenoic acid metabolites							
	Eicosapentaenoic acid	EPA	PUFA	10459.9±4175.6	4259.2±1425.1	0.008	0.035
	9-hydroxy-eicosapentaenoic acid	9-HEPE	NE	4.50±2.72	0.45±0.60	0.009	0.037
	11-hydroxy-eicosapentaenoic acid	11-HEPE	NE	1.06±0.22	0.21±0.10	<0.001	0.001
	18-hydroxy-eicosapentaenoic acid	18-HEPE	NE	1.11±0.22	0.14±0.06	<0.001	0.001
	12-hydroxy-eicosapentaenoic acid	12-HEPE	LOX	42.94±25.80	7.48±9.07	0.005	0.028
	5-hydroxy-eicosapentaenoic acid	5-HEPE	LOX	2.25±0.64	0.17±0.11	<0.001	0.001
	15-hydroxy-eicosapentaenoic acid	15-HEPE	LOX	1.36±0.74	0.07±0.10	0.001	0.009
	14(15)-epoxy-eicosatetraenoic acid	14,15-EpETE	P450	0.72±0.23	0.18±0.10	0.001	0.007

MECH- mechanism; STD – standard diet; HFD- high-fat diet; PUFA – polyunsaturated fatty acid; COX –cyclooxygenase; LOX –lipoxygenase; P450-cytochrome P450; NE- non-enzymatic degradation. All values are pmol/ml plasma expressed as mean ± SD.

Table 5 represents the trends in the kidney and urine of highly correlated metabolites using principal component (PC) analysis

Variable	PC variables	PC Variance	ANOVA p-value	Post Hoc p-values	
			All	STD vs. HFD	HFD vs. HFDAICAR
KIDNEY					
Arachidonic acid					
LOX	15	64.2	0.02	0.03	1
COX	15	45.0	0.81	1	1
P450	17	49.7	0.09	0.11	1
13 PGR	2	60.6	0.06	0.11	1
NE	3	42.2	0.20	0.34	1
Eicosopentaenoic acid					
LOX	3	93.0	0.00002	0.00008	1
NE	2	77.9	0.0000003	0.000001	1
Docosahexaenoic acid					
LOX	4	77.2	0.007	0.006	0.28
COX	2	96.0	0.001	0.001	0.03
P450	2	97.5	0.003	0.003	0.08
NE	4	95.8	0.008	0.007	0.12
Dihomo-γ-linolenic acid					
LOX	2	92.5	0.03	0.06	1
Linoleic acid					
LOX	2	98.0	0.07	0.40	1
NE	2	77.4	0.06	0.42	1
Alpha-Linolenic acid					
LOX	3	82.4	0.26	0.89	0.33
URINE					
Arachidonic acid					
LOX	28	46.3	0.06	0.42	0.95
COX	27	33.6	0.0005	0.004	1
P450	19	53.9	0.12	0.70	1
13 PGR	3	47.7	0.03	0.04	1
PGDH	5	45.6	0.00000002	0.00000001	0.00003
NE	3	48.5	0.002	0.001	0.09
Eicosopentaenoic acid					
LOX	3	96.8	0.14	0.214	0.33
COX	5	50.8	0.00022	0.000161	0.03
CYP	2	82.0	0.85	1	1
NE	3	82.2	0.05	0.24	0.06
Docosahexaenoic acid					
LOX	6	55.0	0.49	0.94	1
COX	2	96.0	0.83	1	1
NE	4	71.3	0.85	1	1
Dihomo-γ-linolenic acid					

LOX	2	97.1	0.02	0.03	1
Linoleic acid					
LOX	2	98.0	0.07	0.4	1
NE	2	77.4	0.04	0.36	0.72
Alpha-Linolenic acid					
LOX	3	82.4	0.26	0.88	0.33
Adrenic acid					
COX	2	71.3	0.00002	0.00002	0.006

PC principal components; PC variables -number of eicosanoids in the principal component; PC variance- amount of variance explained by the principal component; ANOVA p-value- p-value generated comparing all three groups; STD – standard diet; HFD- high-fat diet; HFD+AICAR -high-fat diet and AICAR therapy; COX – cyclooxygenase; LOX –lipoxygenase; P450-cytochrome P450; 13 PGR - delta13-15-ketoprostaglandin reductase; PGDH-15-hydroxyprostaglandin dehydrogenase; NE- non-enzymatic degradation; Red highlight elevated with HFD; Green highlight decreased with HFD; Yellow highlight elevated with AICAR; Blue highlight decreased with AICAR.

Table 6 represents the trends in the arterial and venous blood of highly correlated metabolites using principal component (PC) analysis

Variable	PC variables	PC Variance	ANOVA p-value	Post Hoc p-values	
			All	STD vs. HFD	HFD vs. HFDAICAR
ARTERY					
Arachidonic acid					
LOX	9	40.9	0.73	1	1
13 PGR	2	70.3	0.42	0.60	1
COX	6	59.9	0.90	1	1
P450	13	49.3	0.13	0.43	0.16
Eicosopentaenoic acid					
LOX	3	78.9	0.000003	0.00004	0.72
Docosahexaenoic acid					
LOX	2	79.9	0.001	0.003	1
P450	2	78.1	0.01	0.03	1
NE	4	77.1	0.01	0.01	1
Linoleic acid					
NE	2	92.8	0.32	0.43	0.97
Alpha-Linolenic acid					
LOX	3	75.7	0.04	0.03	0.37
VEIN					
Arachidonic acid					
LOX	8	59.4	0.87	1	1
13 PGR	2	50.5	0.06	0.06	0.47
COX	5	67.2	0.84	1	1
P450	15	47.9	0.12	1	0.19
Eicosopentaenoic acid					
LOX	3	78.0	0.00002	0.00003	0.60
NE	2	82.4	0.00004	0.0003	1
Docosahexaenoic acid					
LOX	3	58.0	0.0004	0.002	1
NE	3	73.9	0.08	0.09	0.76
Linoleic acid					
NE	2	90.4	0.11	0.79	0.11
Alpha-Linolenic acid					
LOX	3	73.7	0.02	0.03	0.09

PC principal components; PC variables -number of eicosanoids in the principal component; PC variance- amount of variance explained by the principal component; ANOVA p-value- p-value generated comparing all three groups; STD – standard diet; HFD- high-fat diet; HFD+AICAR -high-fat diet and AICAR therapy; COX – cyclooxygenase; LOX –lipoxygenase; P450-cytochrome P450; 13 PGR - delta13-15-ketoprostaglandin reductase; PGDH-15-hydroxyprostaglandin dehydrogenase; NE- non-enzymatic degradation; Green highlight demonstrates decreased with HFD.

Figure 1

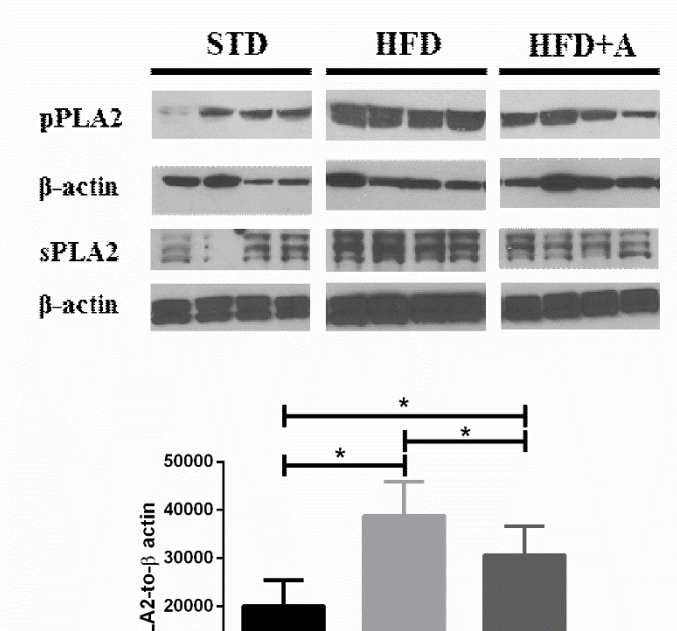

Figure 1. High-fat diet increases cytosolic phospholipase A2 and secretory-phospholipase A2 levels in the mouse kidney that is improved with AICAR treatment. Western blot analysis of the effect of standard (STD), high-fat diet (HFD) and HFD with AICAR (HFD+AICAR) treatment on cytosolic phospho-phospholipase A2 (pPLA2) and secretory- phospholipase A2 (sPLA2) in mice kidney. Relative densitometry of the immunoblots were normalized with beta-actin. Values are means ± SD. N=5 in each group. *p<0.05.

Figure 2

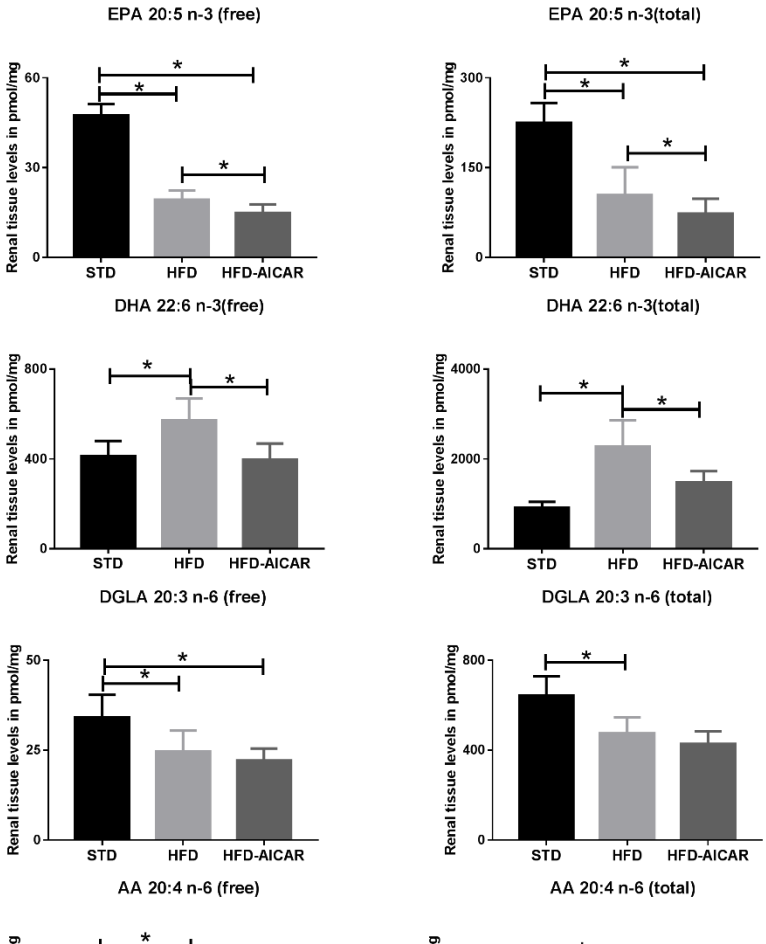

Figure 2. High fat diet increases free and total polyunsaturated fatty acid levels in the mouse kidneys that is rescued by AMPK activation

Total and free levels of ω3 fatty acids eicosapentaenoic acid (EPA, panels A and B) and docosahexaenoic acid (DHA, panels C and D) and ω6 fatty acids – dihommo gamma-linolenic acid (DGLA, panels E and F) and arachidonic acid (AA, panels G and H) in the mice fed standard (STD), high fat diet (HFD), and HFD with AICAR. Values are means ± SD. N=6 in each group. *p<0.05

Figure 3

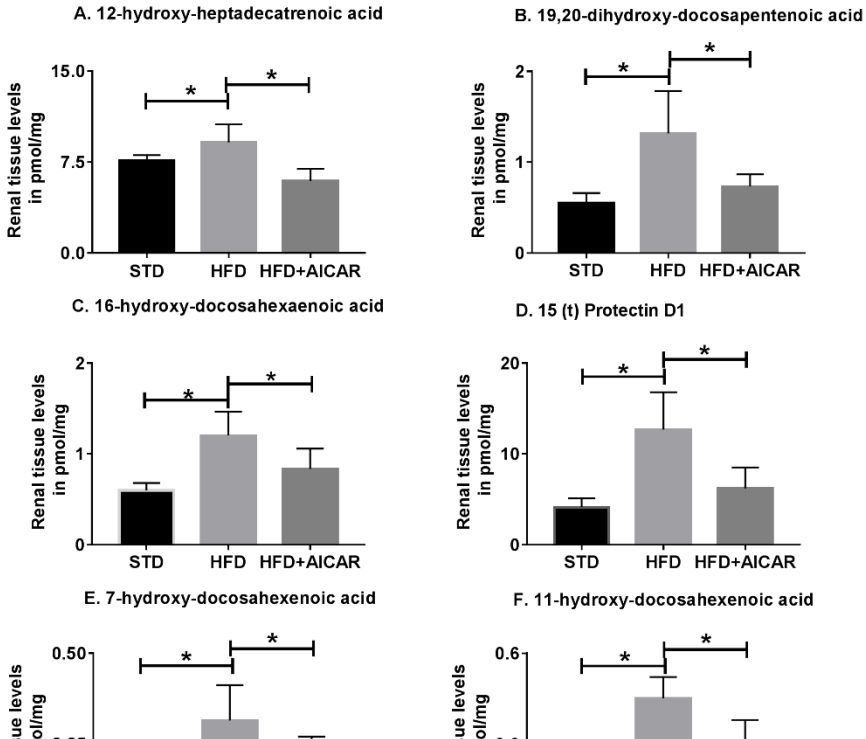

Figure 3. **Profile of eicosanoid species modulated by high-fat diet and AMPK activation in mouse kidneys.**

Eicosanoids profiles show changes in the kidneys of mice fed standard (STD), high-fat diet (HFD), and HFD with AICAR. Values are means ± SD. N=6 in each group. Statistical analyses were performed by one-way ANOVA followed by Fisher post hoc tests. All p values corrected for Bonferroni FDR correction of *q ≤ 0.05. Arachidonic acid metabolite of cytochrome P450 12-hydroxyl-hexadecatrienoic acid (12HHT; Panel A); Docosahexaenoic acid metabolites of cytochrome P450: 19,20-dihydroxy-

docosapenatenoic acid (19,20-DHDPA, Panel B); 16-hydroxy-docosahexaenoic acid (16-HDoHE; Panel C); Lipoxygenase metabolites: 15 (t) Protectin D1 (15(t)-PD1, Panel D), 7-hydroxy-docosahexaenoic acid (7-HDoHE; Panel E), and 11-hydroxy-docosahexaenoic acid (11-HDoHE; Panel F); and non-enzymatic process: 8-hydroxy-docosahexaenoic acid (18-HDoHE; Panel G) and 13-hydroxy-docosahexaenoic acid (13-HDoHE; Panel H).

Figure 4

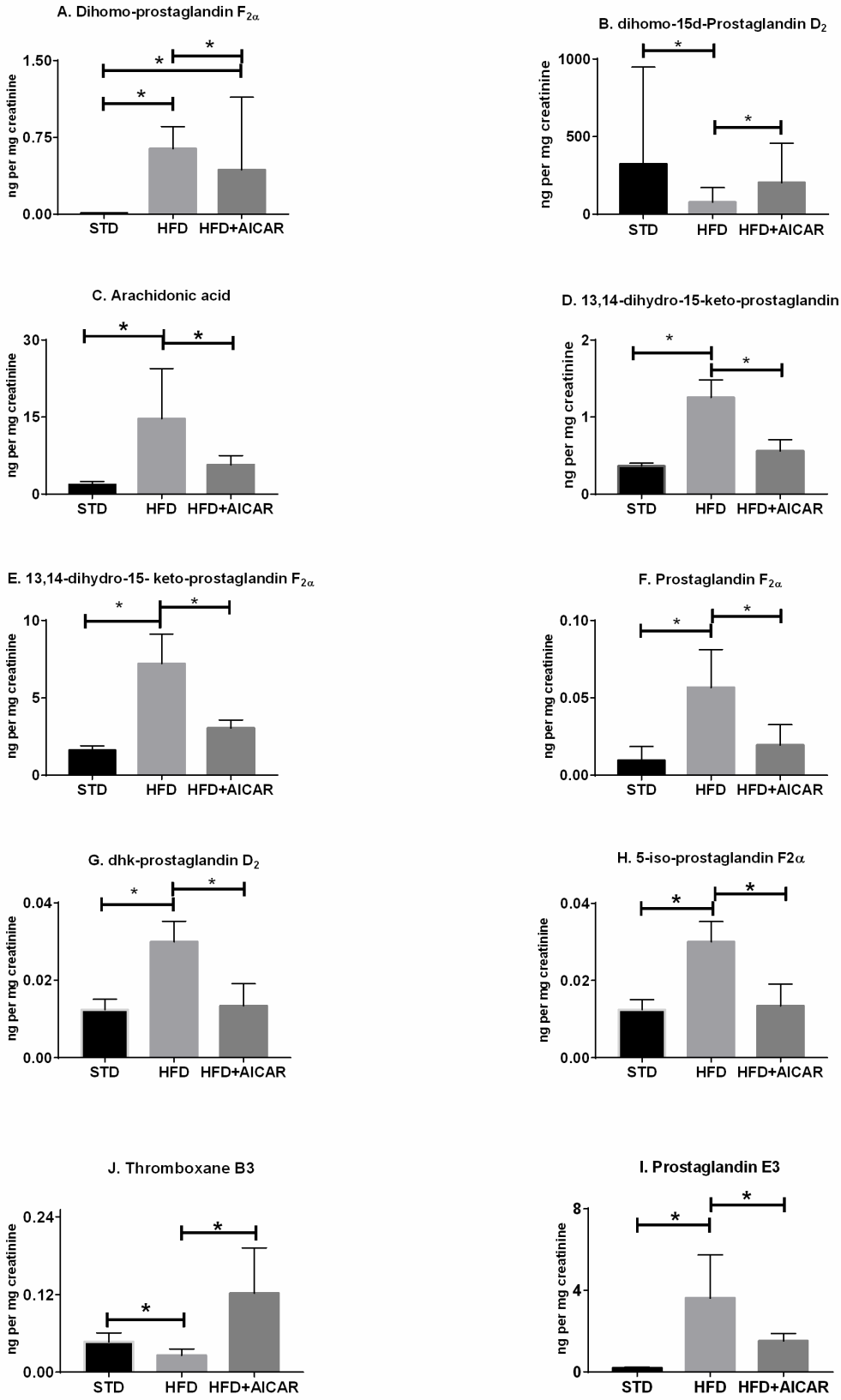

Figure 4. Profile of urinary eicosanoid species in mice on high-fat diet and AICAR.

Eicosanoid species in urine were normalized for concentration with creatinine levels in standard diet (STD), high-fat diet (HFD) and HFD with AICAR therapy. Values are means ± SD of original data or normalized data (log transformed, auto scaled) represented as box plots with whiskers (median, Interquartile interval). N=6 in each group. Statistical analyses were performed by one-way ANOVA by Fisher post hoc tests. All p values corrected for Bonferroni FDR correction of *q ≤ 0.05. Adrenic acid metabolites- dihomo-prostaglandin $PGF_{2\alpha}$ (dihomo-$PGF_{2\alpha}$, Panel A), dihomo-15-deoxyprostaglandin D_2 (dihomo-15d-PGD_2, Panel B). Urine arachidonic acid (AA, Panel C) and its cyclooxygenase metabolites- 13,14-dihydro-15-keto-prostaglandin E_2 (PGEM, Panel D); 13,14-dihydro-5-keto-prostaglandin $F_{2\alpha}$ (PGFM, Panel E); Prostaglandin $F_{2\alpha}$ ($PGF_{2\alpha}$, Panel F); 13,14-dihydro-15-keto-prostaglandin D_2 (dhk-PGD_2, Panel G); non-enzymatic product 5-iso-prostaglandin $F_{2\alpha}$-VI (5-iso-$PGF_{2\alpha}$-VI, Panel H). Cyclooxygenase metabolites of eicosapentaenoic acid- Prostaglandin E_3 (PGE_3, Panel I) and Thromboxane B_3 (TXB_3, Panel J).

Figure 5

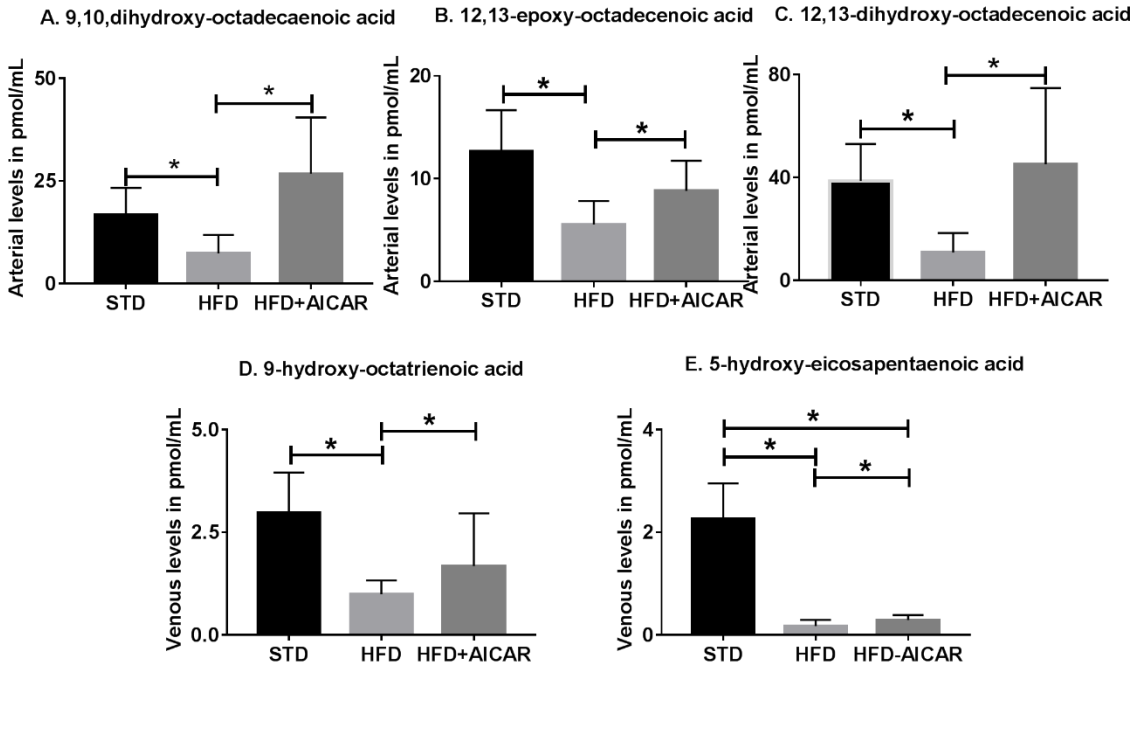

Figure 5. Profile of eicosanoid species in the circulation regulated by high-fat disease and AICAR.

Profile of eicosanoid species in arterial and venous circulation in mice fed a standard diet (STD), high-fat diet (HFD) or HFD with AICAR therapy. Values are means ± SD. N=6 in each group. Statistical analyses were performed by one-way ANOVA followed by Fisher post hoc tests. All p values corrected for Bonferroni FDR correction of *q ≤ 0.05. Linoleic acid metabolites of cytochrome P450 in the artery- 9,10-dihydroxy-octadecaenoic acid (9, 10-diHOME, Panel A), 12,13-epoxy-octadecenoic acid (12,13-EpHOME, Panel B), and 12,13-dihydroxy-octadecenoic acid (12,13-diHOME, Panel C). Venous Lipoxygenase metabolite of alpha-linolenic acid- 9-hydroxy-octatrienoic acid (9-HOTrE, Panel D) and eicosapentaenoic acid- 5-hydroxy-eicosapentaenoic acid (5-HEPE, Panel E).

Figure 6. Schematic diagram of the eicosanoid metabolites regulated by AMPK activation to reverse the effects of high-fat diet in the kidney, urine, arterial and venous circulation.

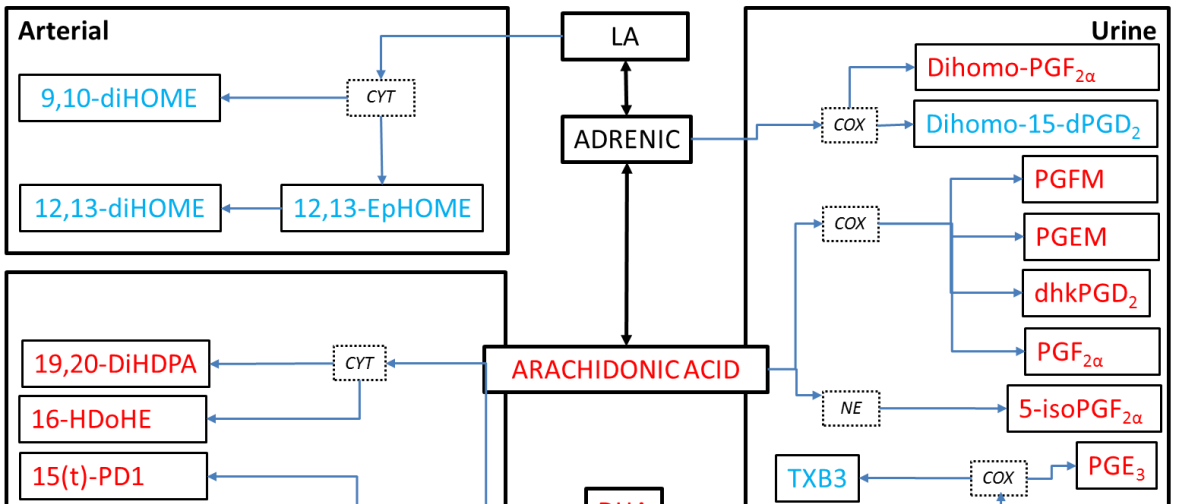

Adrenic acid metabolites-dihomo-prostaglandin $PGF_{2\alpha}$ (dihomo-$PGF_{2\alpha}$) and dihomo-15-deoxy prostaglandin D_2 (dihomo-15d-PGD_2); Arachidonic acid (AA) metabolites-13,14-dihydro-15-keto-prostaglandin E_2 (PGEM) and 13,14-dihydro-5-keto-prostaglandin $F_{2\alpha}$ (PGFM), and Prostaglandin $F_{2\alpha}$ ($PGF_{2\alpha}$); Eicosapentaenoic acid (EPA) metabolites -Prostaglandin E_3 (PGE_3), Thromboxane B_3 (TXB_3) and 5-hydroxy-eicosapentaenoic acid (5-HEPE); Alpha – Linolenic acid (ALA) metabolite- 9-hydroxy-octatrienoic acid (9-HOTrE); Docosahexaenoic acid (DHA) metabolites-19,20-dihydroxy-docosapentenoic acid (19,20-DiHDPA),16-hydroxy-docosahexanoic acid (16-HDoHE), 15 (t)- Protectin D1(15(t)-PD1), 7-hydroxy-docosahexaenoic acid (7-HDoHE), 11-hydroxy-docosahexanoic acid (11-HDoHE), 8-hydroxy-docosahexanoic acid (8-HDoHE); 13-hydroxy docosahexaenoic acid (13-HDoHE); and finally Linoleic

acid metabolite-9,10-dihydroxy-octadecaenoic acid (9,10-diHOME); 12,13, Epoxy-octadecaenoic acid (12,13-EpOME) and, 12,13,dihydroxyoctadecenoic acid (12,13-diHOME). P450- cytochrome P450; LOX – lipoxygenases; COX – cyclooxygenase; NE –non-enzymatic. Red font indicates that high-fat diet increases these metabolites and AICAR reverses this, while blue font indicates the metabolite is decreased with high-fat diet and AICAR reverses this trend.